IPPP/03/51
DCPT/03/102
4 December 2003

arXiv:hep-ph/0311023v2 4 Dec 2003

Extending the study of the Higgs sector at the LHC by proton tagging

A.B. Kaidalov[a,b], V.A. Khoze[a,c], A.D. Martin[a,d] and M.G. Ryskin[a,c]

[a] Department of Physics and Institute for Particle Physics Phenomenology, University of Durham, DH1 3LE, UK
[b] Institute of Theoretical and Experimental Physics, Moscow, 117259, Russia
[c] Petersburg Nuclear Physics Institute, Gatchina, St. Petersburg, 188300, Russia
[d] Department of Physics, University of Canterbury, Christchurch, New Zealand

Abstract

We show that forward proton tagging may significantly enlarge the potential of studying the Higgs sector at the LHC. We concentrate on Higgs production via central exclusive diffractive processes (CEDP). Particular attention is paid to regions in the MSSM parameter space where the partial width of the Higgs boson decay into two gluons much exceeds the SM case; here the CEDP are found to have special advantages.

1 Introduction

The Higgs sector is (so far) an elusive basic ingredient of the fundamental theory of particle interactions. Searches for Higgs bosons, and the study of their properties, are one of the primary goals of the Large Hadron Collider (LHC) at CERN, which is scheduled to commence taking data in the year 2007. The conventional folklore is that (under reasonable model assumptions) at least one Higgs boson should be discovered at the LHC. In particular, if the light Higgs predicted by the Standard Model (SM) exists[1], it will almost certainly be found at the LHC in the first years of running or even maybe before, at the Tevatron. Moreover the LHC should provide a complete coverage of the SM Higgs mass range.

However there is a strong belief that the Standard Model, in its minimal form with a single Higgs, cannot be the fundamental theory of particle interactions. Various extended models predict a large diversity of Higgs-like bosons with different masses, couplings and even CP-parities. The most elaborated extension of the Standard Model is, currently, the Minimal Supersymmetric Standard Model (MSSM) in which there are three neutral (h, H and A) and two charged (H^+, H^-) Higgs bosons, where h and H are CP-even ($m_h < m_H$) and A is CP-odd.

[1] The theoretical progress in the calculations of the signal and background processes has been enormous in recent years, reaching an accuracy of the next-to-next-to-leading QCD corrections for some relevant cross sections, see for example [1] and references therein. At the same time, experimentally related issues of the Higgs search physics have been thoroughly investigated, see for example [2].

Just as for the Standard Model, this benchmark SUSY model has been studied in great detail; for a recent review see [3]. In the MSSM, the properties of the Higgs sector are characterized by the values of two independent input parameters, typically chosen to be the pseudoscalar Higgs boson mass, m_A, and the ratio, $\tan\beta$, of the vacuum-expectation-values of the two Higgs doublet fields. At tree level, the pseudoscalar A does not couple to the gauge bosons and its couplings to down- (up-) type fermions are (inversely) proportional to $\tan\beta$. Within the MSSM, the mass of the h-boson is bounded to $m_h \lesssim 135$ GeV (see, for example, [4] and references therein), while the experimental 95% CL lower limit for a neutral scalar Higgs is $m_h \simeq m_A \sim 92$ GeV [5].

Beyond the Standard Model the properties of the neutral Higgs bosons can differ drastically from SM expectations. In some extended models, the limit for a neutral Higgs can go down to below 60 GeV. This occurs, for instance in the MSSM with explicit CP-violation, where the mass eigenstates of the neutral Higgs bosons do not match the CP eigenstates h, H, A, see, for example, [6]. Further examples are the models with extra dimensions where a Higgs can mix with the graviscalar of the Randall–Sundrum scenario [7], which is called the radion (see for example [8]). In the latter case, due to the trace anomaly, the gluon–gluon coupling is strongly enhanced, which makes this graviscalar especially attractive for searches in gluon-mediated processes, assuming that the background issues can be overcome. These extended scenarios would complicate the study of the neutral Higgs sector using the conventional (semi)inclusive strategies.

After the discovery of a Higgs candidate the immediate task will be to establish its quantum numbers, to verify the Higgs interpretation of the signal, and to make precision measurements of its properties. The separation and identification of different Higgs-like states will be especially challenging. It will be an even more delicate goal to establish the nature of a newly-discovered heavy resonance state. For example, how can one discriminate between the Higgs of the extended SUSY sector from the graviscalar of the Randall–Sundrum scenario (or, even worse, from a mixture of the Higgs and the radion). As was shown in [9], the central exclusive diffractive processes (CEDP) at the LHC can play a crucial role in solving these problems, which are so vital for the Higgs physics. These processes are of the form

$$pp \to p + \phi + p, \tag{1}$$

where the + signs denote the rapidity gaps on either side of the Higgs-like state ϕ. They have unique advantages as compared to the traditional non-diffractive approaches [10, 11]. These processes allow the properties of ϕ to be studied in an environment in which there are no secondaries from the underlying events. In particular, if the forward protons are tagged, then the mass of the produced central system ϕ can be measured to high accuracy by the missing mass method. Indeed, by observing the forward protons, as well as the $\phi \to b\bar{b}$ pairs in the central detector, one can match two simultaneous measurements of the ϕ mass: $m_\phi = \Delta m_{\rm missing}$ and $m_\phi = m_{b\bar{b}}$. Moreover, proton taggers allow the damaging effects of multiple interactions per bunch crossing (pile-up) to be suppressed and hence offer the possibility of studying CEDP processes at higher luminosities [11]. Thus the prospects of the precise mass determination of the Higgs-like states, and even of the direct measurements of their widths and $\phi \to b\bar{b}$ couplings, looks feasible using these processes. A promising option is to use the forward proton taggers as a spin-parity analyser [9]. This may provide valuable additional (and in some cases unique) information in the unambiguous identification of a newly discovered state.

In Section 2 we illustrate the advantages of CEDP, (1), in exploring the Higgs sector in specific parameter ranges of the MSSM. First in Section 2.1 we consider the so-called "intense-coupling" regime [12, 13] where the $\gamma\gamma$, $WW^\star$ and $ZZ^\star$ Higgs decay modes are suppressed but where, on the other hand, the CEDP cross section is enhanced, in comparison with the SM. Next, in Section 2.2, we discuss the decoupling limit ($m_A > 2M_Z$, $\tan\beta > 5$) where the light scalar, h, looks very similar to the SM Higgs. In this case the discovery of the heavier scalar H is crucial to establish the underlying structure of the electroweak-symmetry-breaking dynamics. If $m_H < 250$ GeV, then the H boson may be observed and studied in CEDP. In Section 2.3 we show that CEDP may cover the "windows" where, once the h boson is discovered, it is not possible to disentangle the H or A bosons by traditional means. In Section 3 we explain how studies of CEDP may help to determine the properties of the Higgs-like states, once they have been discovered.

The plan of the paper is first to present the predictions and then, in Section 4, to explain how the cross sections for the CEDP of the ϕ CP-even and CP-odd Higgs states are calculated. In this Section we also enumerate the uncertainties in the predictions. Simple formulae to approximate the CEDP cross sections for

$pp \to p + \phi + p$ with $\phi \to b\bar{b}$, and the corresponding QCD $b\bar{b}$ background, are given in Section 5. These allow quick, reliable estimates to be made of the signal-to-background ratio for a Higgs of any mass, and both CP parities.

In Section 6 we focus attention on ways to identify the pseudoscalar boson A. It is unlikely that the pure exclusive diffractive production process will have sufficient events, and so possible semi-inclusive signals are proposed and studied.

2 Discovery potential of diffractive processes

The main aim of this paper is to show how the Higgs discovery potential at the LHC may be enlarged by using the unique advantages of forward proton tagging. Special attention is paid to the cases where the partial widths for the decay of Higgs bosons into two gluons greatly exceed the SM values. As mentioned above, we shall illustrate the advantages of using forward proton tagging to study the Higgs sector by giving predictions for a few examples within the MSSM model.

2.1 The intense coupling regime

The "intense-coupling regime" [12, 13] is where the masses of all three neutral Higgs bosons are close to each other and the value of $\tan\beta$ is large. Then the $\gamma\gamma, WW^\star, ZZ^\star$ decay modes (which are among the main detection modes for the SM Higgs) are strongly suppressed. This is the regime where the variations of all MSSM Higgs masses and couplings are very rapid. This region is considered as one of the most challenging for the (conventional) Higgs searches at the LHC, see [13] and references therein. On the other hand, here the CEDP cross sections are enhanced by more than an order of magnitude (due to the large $gg \to \phi$ couplings). Therefore the expected significance of the CEDP signal becomes quite large. Indeed, this is evident from Fig. 1, which shows the cross sections for the CEDP production of h, H, A bosons as functions of their mass for $\tan\beta = 30$ and 50. The cross sections are computed as described in Section 5, with the widths and properties of the Higgs scalar (h, H) and pseudoscalar (A) bosons obtained from the HDECAY code, version 3.0 [15], with all other parameters taken from Table 2 of [15]; also we take IMODEL = 4, which means the radiative corrections are included according to Ref. [16].

Let us focus on the main $\phi \to b\bar{b}$ decay mode[2]. This mode is well suited for CEDP studies, since a P-even, $J_z = 0$ selection rule [18, 19, 20] suppresses the QCD $b\bar{b}$ background at LO. Indeed, at the LHC, the signal-to-background ratio is $S/B \sim 3$ for a Standard Model Higgs boson of mass $m = 120$ GeV, if the experimental cuts and efficiencies quoted in [11] are used. This favourable ratio was obtained since it was argued that proton taggers can achieve a missing mass resolution of $\Delta m_{\rm missing} \simeq 1$ GeV. Due to the enhancement of the production of MSSM scalars, for large $\tan\beta$, the QCD background becomes practically negligible. Note that, normally, to estimate the statistical significance of the measurement of the signal cross section, we use the conservative formula $\sqrt{S+B}$ for the statistical error. However when we are looking for a new particle, which gives some peak on the top of the background, the statistical error may be much lower. It is given just by the fluctuation of the background – $\sqrt{B}$. On the other hand for a low number of events, it is appropriate to use a Poisson, rather than a Gaussian, distribution. Thus the statistical significance to discover a new particle has to be evaluated more precisely. For instance, with the cuts and efficiencies quoted in [11], we estimate that the QCD background is $B = 40(4)$ events for an integrated luminosity of $\mathcal{L} = 300$ fb^{-1} (30 fb^{-1}), if we take $M = 120$ GeV and $\Delta M = 1$ GeV. Thus, to obtain a confidence coefficient of 5.7×10^{-7} (equivalent to a statistical significance of 5σ for a Gaussian distribution[21]), it is sufficient for the cross section of a Higgs signal, times the $b\bar{b}$ branching fraction, to satisfy

$$\mathrm{Br}(b\bar{b}) \cdot \sigma > 0.7 \text{ fb } (2.7 \text{ fb}) \tag{2}$$

[2]The exclusive diffractive studies in Ref. [11] addressed mainly the $b\bar{b}$ decay mode. The use of the $\tau\tau$ decay mode requires an evaluation of the $pp \to p + \tau\tau + p$ background, especially of the possibility of misidentifying gluon jets as τ's in the CEDP environment. Currently, for inclusive processes, the probability, $P(g/\tau)$, to misidentify a gluon as a τ is estimated to be about 0.002 [17].

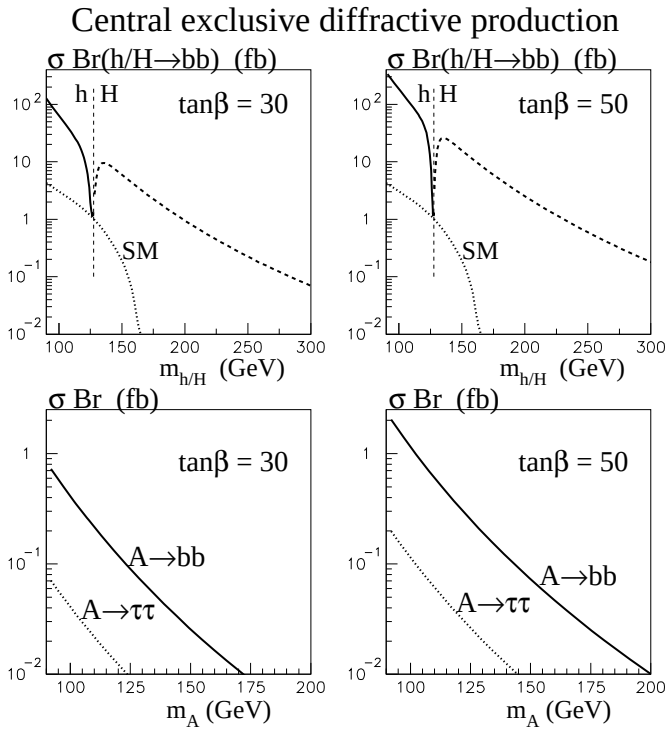


Figure 1: The cross sections, times the appropriate $b\bar{b}$ and $\tau^+\tau^-$ branching fractions, predicted for central exclusive diffractive production of $h(0^+)$, $H(0^+)$ and $A(0^-)$ MSSM Higgs bosons (for $\tan\beta = 30$ and 50) at the LHC, obtained using the MRST99 [14] gluon distribution. The dotted curve in the upper plots shows the cross section for the production of a SM Higgs boson. The vertical line separates the mass regime of light $h(0^+)$ and heavy $H(0^+)$ bosons. The curves were computed using version 3.0 of the HDECAY code [15], with all other parameters taken from Table 2 of [15]; the radiative corrections were included according to Ref. [16].

if we take the integrated luminosity to be $\mathcal{L} = 300$ fb^{-1} (30 fb^{-1}).

As can be seen from Fig. 1, for MSSM with $\tan\beta = 50$ the expected CEDP cross section times branching fraction, $\mathrm{Br}(H \to b\bar{b})\sigma_H$, is greater than 0.7fb for masses up to $m_H \sim 250$ GeV. The situation is worse for pseudoscalar, A, production, since the cross section is suppressed by the P-even selection rule. Thus the CEDP filters out pseudoscalar production, which allows the possibility to study pure H production, see Fig. 1. This may be also useful in the decoupling limit, to which we now turn.

2.2 The decoupling limit

For $m_A > 2m_Z$ and $\tan\beta > 5$, there is a wide domain in MSSM parameter space where the light scalar h becomes indistinguishable from the SM Higgs, and the other two neutral Higgs states are approximately degenerate in mass. This is the so-called decoupling limit [22]. Moreover in many theories with a non-minimal Higgs sector, there are significant regions of parameter space that approximate the decoupling limit; see, for instance, [3]. In this regime the discovery of the heavier non-minimal Higgs scalar H is crucial for establishing the underlying structure of the electroweak-symmetry-breaking dynamics. Here, forward proton tagging can play an important role in searching for (at least) the H-boson, if it is not too heavy ($m_H \lesssim 250$ GeV). For large values of $\tan\beta$ the decoupling regime essentially starts at $m_A \simeq 170$ GeV. As can be seen in Fig. 1, the cross section is still sufficiently large to ensure the observation of the H boson up to $m_A \simeq 250$ GeV. To illustrate the moderate $\tan\beta$ region we consider the case $m_A = 185$ GeV and $\tan\beta = 7$. Then the CEDP cross section is

$$\mathrm{Br}(H \to b\bar{b})\sigma_H = 0.17 \text{ fb}. \tag{3}$$

Thus for an integrated luminosity of $\mathcal{L} = 300$ fb^{-1} we have about 8.5 events, after applying the experimental cuts and efficiencies discussed in Ref. [11]. The corresponding background is about 2.6 events. Using again a Poisson distribution, as we did in the case of (2), then the expected statistical significance to observe such an H boson is about 4σ. So detection may be feasible.

The possibility to use exclusive diffractive processes to explore larger masses will depend on various experiment-related factors. In particular, on the prospects to achieve better mass resolution, Δm, at higher mass, m.

2.3 The 'window' or 'hole' regions

There are regions of MSSM parameter space where, after the h boson is discovered, it will be difficult to identify the heavy H or A bosons by conventional non-diffractive processes. Can the CEDP processes help here? First consider the 'notorious hole' in parameter space (sometimes called the "LHC wedge"), defined by $m_A \gtrsim 200$ GeV and $\tan\beta \sim 4$–7 [3]. In this region, only the lightest Higgs h can be discovered even with integrated luminosity of the order of 300 fb^{-1}. Its properties are nearly indistinguishable from those of a SM Higgs. Unfortunately here, even for H, the predicted CEDP cross section is too low, assuming the efficiencies and cuts of Ref. [11]; see the heavy continuous curve in Fig. 2.

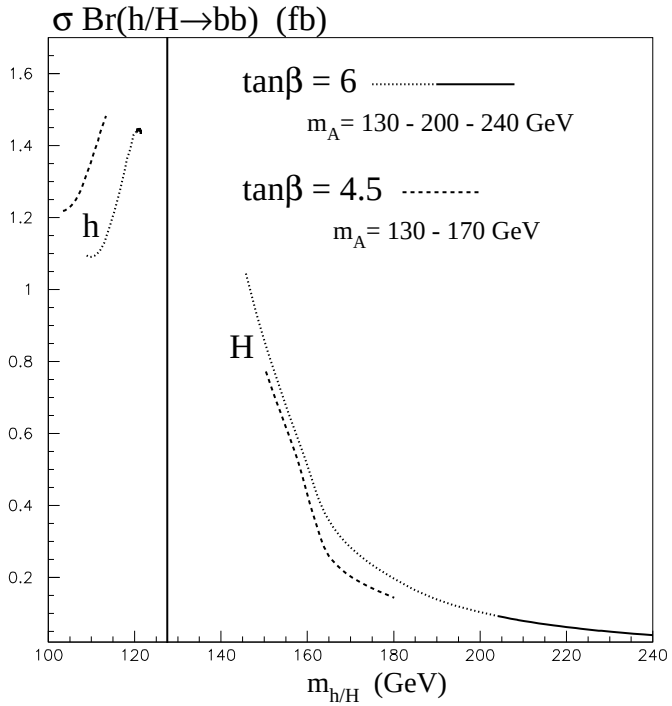


Figure 2: The cross sections for the central exclusive diffractive production of h and H bosons, $pp \to p+(h,H)+p$, times the appropriate $b\bar{b}$ branching fraction, as a function of their mass, in two regions of MSSM parameter space where observation of the H using non-diffractive processes is difficult. Note that in the first region the curve changes from dotted to continuous when the mass of the $A(0^-)$ bosons reaches 200 GeV; and that the value of m_h is practically unchanged for values of m_A in the region $m_A > 200$ GeV.

However, with the present understanding of the capabilities of the detectors it is plausible that similar windows will occur in the interval $130 \lesssim m_A \lesssim 170$ GeV for $\tan\beta \simeq$4–6.[3] That is, it may be impossible to identify the H scalar by conventional processes at the 5σ confidence level with 300 fb^{-1} of combined ATLAS+CMS luminosity. From the predictions shown by the dashed line in Fig. 2, we see that the part of this 'hole', up to

[3]We are grateful to Sasha Nikitenko for pointing out the importance of the additional (nonconventional) studies in this region.

$m_H \sim 160$ GeV, may be covered by CEDP. For illustration, consider the case $m_H = 150$ GeV and $\tan\beta = 4.5$. With an integrated luminosity of $\mathcal{L} = 300$ fb^{-1}, the CEDP cross section of

$$\mathrm{Br}(H \to b\bar{b})\sigma_H = 0.8 \text{ fb} \tag{4}$$

gives about 40 events, after applying the experimental cuts and efficiencies discussed in Ref. [11]. The corresponding background is about 10 events. Thus, if we use a Poisson distribution, as we did in the case of (2), then the expected statistical significance to observe such an H boson will exceed 10σ.

2.4 Exotic scenarios

Recently some interesting applications of the CEDP to studies of the more exotic Higgs scenarios, such as models with CP violation and searches for the radions, have been discussed [23]. However the feasibility of applying these studies will require further critical discussion of the background issues.

3 Potential of diffractive processes after a Higgs discovery

As was discussed in Refs. [11, 9], the use of CEDP, with forward proton tagging, can provide a competitive way to detect a Higgs boson. This approach appears to have special advantages for searches of the CP-even Higgses of MSSM in the intense-coupling regime. Indeed, the CEDP cross section can exceed the SM result by more than an order of magnitude, see Fig. 1. Once a Higgs-like signal is observed, it will be extremely important to verify that it is indeed a Higgs boson. Here we describe where forward proton tagging can provide valuable help to establish the nature of the newly discovered state and to verify whether it can be interpreted as a Higgs boson. We also emphasize that CEDP are well suited to study specific cases which pose difficulties for probing the Higgs sector at the LHC.

It is generally believed that a detailed coverage of the Higgs sector will require complementary research programmes at the LHC and a Linear e^+e^- collider. Interestingly, in some sense, the implementation of forward proton taggers allows some studies which otherwise would have to await the construction of a Linear e^+e^- collider. Moreover, in addition to the other advantages, forward proton tagging offers the possibility to study New Physics in the photon–photon collisions, see for example [24, 25, 26, 10].

As mentioned above, if a candidate Higgs signal is detected it will be a challenging task to prove its Higgs identity. Unlike the conventional inclusive approaches, the very fact of seeing the resonance state in CEDP automatically implies that the newly discovered state has the following fundamental properties. It must have zero electric charge and be a colour singlet. Furthermore, assuming P and C conservation, the dominantly produced state has a positive natural parity, $P = (-1)^J$ and even CP. Recall that the installation of forward proton taggers also allows the attractive possibility of a spin-parity analysis. This may provide valuable additional (and in some cases unique) leverage in establishing the origin of the discovered candidate state. In particular, assuming CP conservation, the CEDP allow the $0^-, 1^-, 1^+$ states to be filtered out, leaving only an ambiguity between the 0^{++} and 2^{++} states. Though without further efforts the 2^{++} state cannot be ruled out, this would not be the most likely choice.

As discussed in [9], studying of the azimuthal correlations of the outgoing protons can allow further spin-parity analysis. In particular, it may be possible to isolate the 0^- state. The azimuthal distribution distinguishes between the production of scalar and pseudoscalar particles [9]. Note that with the forward protons we can determine the CP-properties of the Higgs boson irrespective of the decay mode. Moreover, CEDP allow the observation of the interference effects between the CP-even and CP-odd $gg \to \phi$ transitions (see [27]).

Following the discovery, and the determination of the basic quantum numbers, of the new state, the next step is to check whether the coupling properties match those expected for the Higgs boson. For this, we need to detect the signal in at least two different channels. The CEDP mechanism provides an excellent opportunity [4] to detect the $b\bar{b}$ mode. The other decay channel which is appropriate for CEDP studies is the $\tau\tau$ decay mode (or $WW^\star$, or $\mu\mu$, if the event rate is sufficient). These measurements allow a non-trivial check of the theoretical

[4] Recall that for more inclusive processes the signal is overwhelmed by the QCD $b\bar{b}$ background.

models. For example, the precise measurement of the partial decay widths into tau and bottom quark pairs can provide a way to discriminate between supersymmetric and non-supersymmetric Higgs sectors, and to probe CP-violating effects (for recent papers see, for instance, [28] and references therein).

For illustration, consider the following topical example, namely the intense coupling limit of MSSM. As mentioned before, this regime is especially difficult for conventional inclusive studies of the MSSM Higgs [12, 13]. On the other hand, with forward proton taggers, CEDP offer an ideal probe.

For numerical purposes, we choose the same parameters as in [13], in particular, $\tan\beta = 30$, together with results for $\tan\beta = 50$. The salient features of this regime are that there is almost a mass degeneracy of the neutral Higgs states, and their total widths can be quite large (due to the $\tan^2\beta$ increase) and reach up to 1–2 GeV. This can be seen from Fig. 3, where we plot the mass differences $\Delta M = m_A - m_h$ and $\Delta M = m_H - m_A$, and the widths of the bosons, as a function of the pseudoscalar mass m_A. It is especially difficult to disentangle the

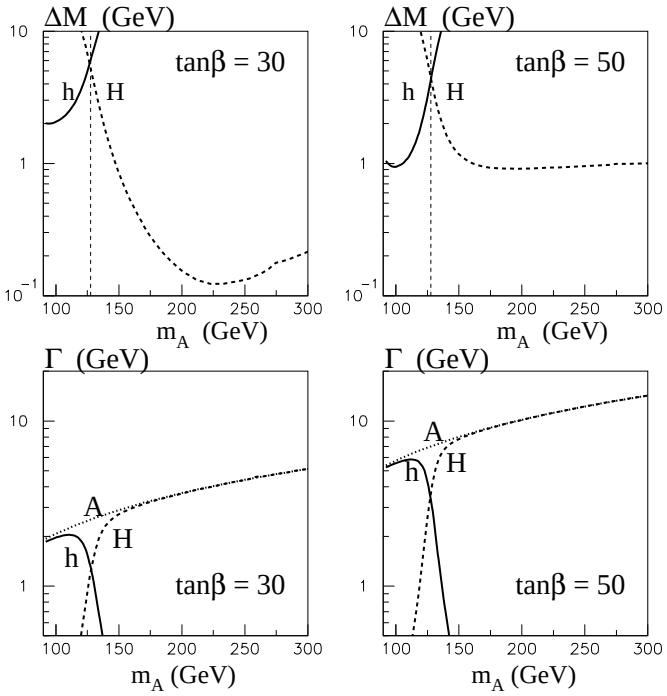


Figure 3: The upper plots show the differences $\Delta M = m_A - m_h$ (continuous curve) and $\Delta M = m_H - m_A$ (dashed curve) as a function of m_A for $\tan\beta = 30$ and 50 respectively. The lower plots show the total widths of the MSSM neutral high bosons.

Higgs bosons in the region around $m_A \sim 130$ GeV, where all three neutral Higgs states practically overlap [13]. Since the traditional non-diffractive approaches do not, with the exception of the $\gamma\gamma$ and $\mu\mu$ modes, provide a mass resolution better than 10–20 GeV, all three Higgs bosons will appear as one resonance[5].

As an example, we give the expected number of CEDP signal and background events for $\mathcal{L} = 30$ fb^{-1} for $m_A = 130$ GeV, using the efficiencies and angular cuts adopted in Ref. [11]. For $\tan\beta = 30(50)$, the number of the $A \to b\bar{b}$ signal events, $S_A = 0.35(1)$, while the QCD background is $B = 2.5$ for $\Delta M = 1$ GeV. For this choice of parameters, $m_h = 122.7(124.4)$ GeV, and the number of the $h \to b\bar{b}$ events is $S_h = 30(71)$ with background $B = 3.5(3.2)$. The corrresponding numbers for the H boson are $m_H = 134.2(133.5)$ GeV, $S_H = 47(124)$ and

[5]Recall that in this regime the $\gamma\gamma$ decay mode is hopeless. Moreover, the vector-boson-fusion Higgs production, with the $b\bar{b}$ or $\tau\tau$ decays, does not allow the separation of the h and H peaks due to the poor invariant mass resolution. As shown in [13], only the detection of the rare dimuon Higgs decay mode may provide a chance to separate the Higgs states in inclusive production. Even this would require that the Higgs mass splitting exceeds at 3–5 GeV.

$B = 2.1$.

An immediate advantage of CEDP, for studying this troublesome region, is that the A contribution is strongly suppressed, while the h and H states can be well separated ($m_H - m_h \simeq 10$ GeV) given the anticipated experimental mass resolution of $\Delta M \sim 1$ GeV [11], see Fig. 4. Note that precision measurements of the two

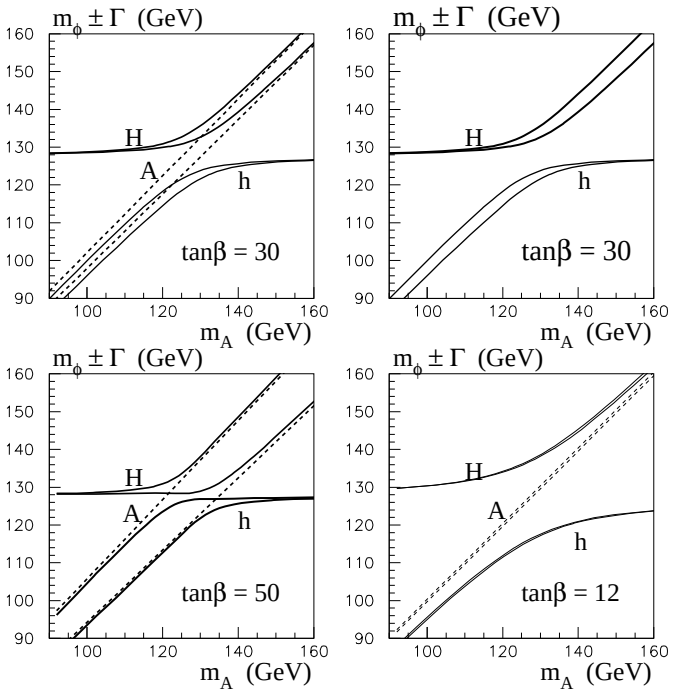


Figure 4: The mass bands $m_\phi \pm \Gamma$ for neutral MSSM Higgs bosons as a function of m_A, for different values of $\tan\beta$. A vertical slice through these plots, at a given value of m_A, indicates the position of the MSSM resonance Higgs peaks. The upper right hand plot shows that the h and H bosons are clearly identifiable for $\tan\beta = 30$, if $A(0^-)$ production is suppressed. The lower plots show how the sensitivity of the widths, to variations of $\tan\beta$, will change the profile of the peaks. This way of presentation was motivated by Ref. [13]. Note that the widths of the bosons for $\tan\beta$ less than about 15 become barely visible on this type of plot.

CP-even Higgs states may allow a direct determination of the basic MSSM parameter, $\tan\beta$.

Moreover, the forward tagging approach can provide a direct measurement of the width[6] of the h (for $m_h \lesssim 120$ GeV) and the H-boson (for $m_H \gtrsim 130$ GeV). Outside the narrow range $m_A = 130 \pm 5$ GeV, the widths of the h and H are quite different (one is always much narrower than the other), see Fig. 3. Recall that the width measurement can play an important role in the understanding of Higgs dynamics. It would be instructive to observe this phenomenon experimentally.

As discussed in [9], for $\tan\beta = 30$ the central exclusive signal should be still accessible at the LHC up to an H mass about 250 GeV. For instance, for $m_H = 210$ GeV, and LHC luminosity 30 fb^{-1} (300 fb^{-1}), about 20 (200) $H \to b\bar{b}$ events are produced. If the experimental cuts and efficiencies quoted in DKMOR are imposed, then the signal is depleted by about a factor of 6. This leaves 3 (30) observable events, with background of about 0.1 (1) events.

[6]Note that, strictly speaking, when the Higgs width, Γ, becomes comparable to the mass resolution, Δm, the zero-width approximation is not valid any more. Therefore in calculations of the cross sections the mass resolution and large-width effects should be taken into account.

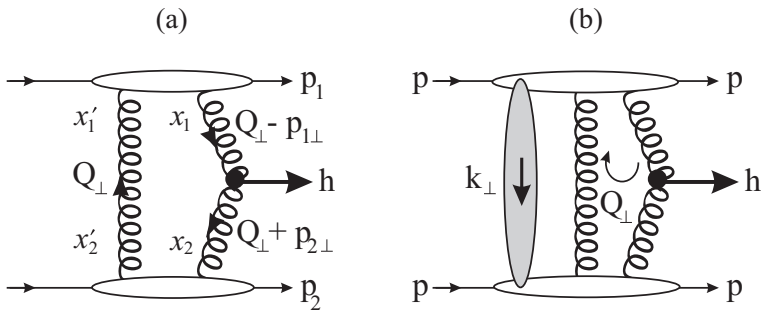


Figure 5: (a) The QCD diagram for double-diffractive exclusive production of a Higgs boson h, $pp \to p+h+p$, where the gluons of the hard subprocess $gg \to h$ are colour screened by the second t-channel gluon. (b) The rescattering or absorptive corrections to $pp \to p+h+p$, where the shaded region represents the soft pp rescattering corrections, leading to the suppression factor S^2.

4 Calculation of the $0^\pm$ Higgs cross sections and their uncertainties

To calculate the cross section for the central exclusive diffractive production of $h(0^\pm)$ Higgs bosons[7] we use the formalism of Refs. [29, 20, 10]. The amplitudes are described by the diagram shown in Fig. 5(a), where the hard subprocesses $gg \to h(0^\pm)$ are initiated by gluon–gluon fusion and where the second t-channel gluon is needed to screen the colour flow across the rapidity gap intervals. Ignoring, for the moment, the screening corrections of Fig. 5(b), the Born amplitudes are of the form [9]

$$T_h = A\pi^2 \int \frac{d^2Q_\perp \; V_h}{Q_\perp^2 (\vec{Q}_\perp - \vec{p}_{1\perp})^2 (\vec{Q}_\perp + \vec{p}_{2\perp})^2} \, f_g(x_1, x_1', Q_1^2, \mu^2; t_1) f_g(x_2, x_2', Q_2^2, \mu^2; t_2), \tag{5}$$

where the $gg \to h(0^\pm)$ subprocesses are specified by [29, 30]

$$A^2 = K \frac{\sqrt{2} G_F}{9\pi^2} \alpha_S^2(m_h^2), \tag{6}$$

with the NLO K factor $K \simeq 1.5$ [31, 10], and by the factors

$$\begin{array}{rcl} V_{h(0^+)} & = & (\vec{Q}_\perp - \vec{p}_{1\perp}) \cdot (\vec{Q}_\perp + \vec{p}_{2\perp}) \\ V_{h(0^-)} & = & \Big((\vec{Q}_\perp - \vec{p}_{1\perp}) \times (\vec{Q}_\perp + \vec{p}_{2\perp}) \Big) \cdot \vec{n}_0 \, . \end{array} \tag{7}$$

Here $\vec{n}_0$ is a unit vector in the beam direction. The f_g's are the skewed unintegrated gluon densities of the proton at the hard scale μ, taken to be $m_h/2$, with

$$\begin{array}{rcl} Q_1 & = & \min \Big\{ Q_\perp, |(\vec{Q}_\perp - \vec{p}_{1\perp})| \Big\} , \\ Q_2 & = & \min \Big\{ Q_\perp, |(\vec{Q}_\perp + \vec{p}_{2\perp})| \Big\} . \end{array} \tag{8}$$

The longitudinal momentum fractions carried by the gluons satisfy

$$\left(x' \sim \frac{Q_\perp}{\sqrt{s}} \right) \ll \left(x \sim \frac{m_h}{\sqrt{s}} \right) \ll 1 \tag{9}$$

where, for the LHC, with $\sqrt{s} = 14$ TeV, we have $x \sim 0.01$, while $x' \sim 10^{-4}$. Below, we assume factorization of the unintegrated distributions,

$$f_g(x, x', Q^2, \mu^2; t) = f_g(x, x', Q^2, \mu^2) F_N(t), \tag{10}$$

[7] For convenience of presentation in this section we denote the pseudoscalar boson by $h(0^-)$ rather than $A(0^-)$.

where we parameterize the form factor of the proton vertex by the form $F_N(t) = \exp(bt)$ with $b = 2$ GeV^{-2}. In the domain specified by (9) the skewed unintegrated densities are given in terms of the conventional (integrated) densities $g(x, Q_i^2)$. To single log accuracy, we have [32][8].

$$f_g(x, x', Q_i^2, \mu^2) = R_g \frac{\partial}{\partial \ln Q_i^2} \left(\sqrt{T(Q_i, \mu)}\, x g(x, Q_i^2) \right), \tag{11}$$

where T is the usual Sudakov form factor which ensures that the gluon remains untouched in the evolution up to the hard scale μ, so that the rapidity gaps survive. This Sudakov factor T is the result of resumming the virtual contributions in the DGLAP evolution. It is given by

$$T(Q_\perp, \mu) = \exp\left(- \int_{Q_\perp^2}^{\mu^2} \frac{\alpha_S(k_t^2)}{2\pi} \frac{dk_t^2}{k_t^2} \int_0^{1-\Delta} \left[z P_{gg}(z) + \sum_q P_{qg}(z) \right] dz \right). \tag{12}$$

Here we wish to go beyond the collinear approximation and in the T factor to resum, not just the single collinear logarithms, but the single soft log $1/(1-z)$ terms as well. Thus we consider the region of large-angle soft gluon emission, and explicitly calculate the one-loop vertex diagram. In particular, we do not approximate $\sin\theta$ by θ. Then we adjust the upper limit of the z integration in (12) to reproduce the complete one-loop result[9]. We find

$$\Delta = \frac{k_t}{k_t + 0.62 m_h}. \tag{13}$$

The square root in (11) arises because the bremsstrahlung survival probability T is only relevant to hard gluons. R_g is the ratio of the skewed $x' \ll x$ integrated distribution to the conventional diagonal density $g(x, Q^2)$. For $x \ll 1$ it is completely determined [33], with an uncertainty in R_g of the order of $4x^2$. The apparent infrared divergence of (5) is nullified[10] for $h(0^+)$ production by the Sudakov factors embodied in the gluon densities f_g. However, as discussed in Ref. [9], the amplitude for $h(0^-)$ production is much more sensitive to the infrared contribution. Indeed let us consider the case of small $p_{i\perp}$ of the outgoing protons. Then, from (7), we see that $V_{h(0^+)} \sim Q_\perp^2$, whereas $V_{h(0^-)} \sim p_{1\perp} p_{2\perp}$ (since the linear contribution in $Q_\perp$ vanishes after the angular integration). Thus the $d^2Q_\perp/Q_\perp^4$ integration for $h(0^+)$ is replaced by $p_{1\perp}p_{2\perp}d^2Q_\perp/Q_\perp^6$ for $h(0^-)$, and now the Sudakov suppression is not enough to prevent a significant contribution from the $Q_\perp^2 \lesssim 1$ GeV^2 domain.

4.1 Uncertainties in predictions of the cross sections

To estimate the uncertainty in the predictions for the $h^\pm(0)$ exclusive diffractive cross sections we first quantify the above uncertainty arising from the infrared region, where the gluon distribution is not well known. As an example, consider $h(0^-)$ and $h(0^+)$ production at the LHC, for $m_h = 120$ GeV and $\mu = m_h/2$, using different treatments of the infrared region. We perform calculations using MRST99 [14] and CTEQ6M [34] partons respectively with the very low Q gluon frozen at its value at $Q_{1,2} = 1.3$ GeV. Then we integrate down in $Q_\perp$ until $Q_{1,2}$ are close to $\Lambda_{\rm QCD}$, where the contribution vanishes due to the presence of the T-factor. This will slightly overestimate the cross sections, as for $x \sim 0.01$ the gluon density has a positive anomalous dimension ($xg \sim (Q^2)^\gamma$ with $\gamma > 0$) and decreases with decreasing Q^2. A lower extreme is to remove the contribution below $Q_{1,2} = 1.3$ GeV entirely. Even with this extreme choice, the 0^+ cross section is not changed greatly; it is depleted by about 20%. On the other hand, as anticipated, for 0^- production, the infrared region is much more important and the cut reduces the cross section by a factor of 5.

Another uncertainty is the choice of factorization scale μ. Note that in comparison with previous calculations [10], which were done in the limit of proton transverse momenta, $p_{1,2\perp} \ll Q_\perp$, now we include the explicit $p_\perp$-dependence in the $Q_\perp$-loop integral of (5). We resum the 'soft' gluon logarithms, $\ln 1/(1-z)$, in

[8] In the actual computations we use a more precise form as given by eq.(26) of Ref.[32]

[9] An explicit computation of the one-loop vertex contribution from the region of gluon transverse momentum $Q_\perp \ll k_\perp \ll m_h/2$ gives $(N_c\alpha_S/\pi)[0.212 + \ln(m_h/2k_\perp) - 11/12]dk_\perp^2/k_\perp^2$. The last number in the square brackets corresponds to the standard non-logarithmic contribution related to the $zP_{gg}(z)$ term in (12), while the first number stems from the exact treatment of large-angle gluon radiation. This result can be incorporated in (12) by simply choosing Δ as in (13).

[10] In addition, at LHC energies, the effective anomalous dimension of the gluon gives an extra suppression of the contribution from the low $Q_\perp$ domain [30].

the T-factor. So now the T-factor includes both the soft and collinear single logarithms. The only uncertainty is the non-logarithmic NLO contribution. This may be modelled by changing the factorization scale, μ, which fixes the maximal k_t of the gluon in the NLO loop correction. As the default we have used $\mu = m_h/2$; that is the largest k_t allowed in the process with total energy m_h. Choosing a lower scale $\mu = m_h/4$ would enlarge the cross sections by about 30%. Recall that the general calculation is performed in the collinear approximation. However, when we take account of large-angle soft gluon emission in the form factor, that is in the calculation of the virtual-loop correction, as in (12) and (13), we go beyond the collinear approximation. The corresponding real contribution in (11) is represented by R_g and the derivative of the $\sqrt{T}$ factor. Strictly speaking, for the case of large-angle emission there will be some small deviation from this simplified formula. This gives an extra uncertainty of the order of 10%.

Next there is some uncertainty in the gluon distribution itself. To evaluate this, we compare predictions obtained using CTEQ6M [34], MRST99 [14] and MRST02 [35] partons. For 0^+ production at the LHC, with $m_h = 120$ GeV and $\mu = m_h/2$, we find that the effective gluon–gluon luminosity, before screening, is

$$\left.\frac{d\mathcal{L}}{dyd\ln m^2}\right|_{y=0} = (2.2,\ 1.7,\ 1.45)\times 10^{-2} \tag{14}$$

respectively. This spread of values arises because the CTEQ gluon is 7% higher, and the MRST02 gluon 4% lower, than the default MRST99 gluon, in the relevant kinematic region. The sensitivity to the gluon arises because the central exclusive diffractive cross section is proportional to the 4th power of the gluon. For 0^- production, the corresponding numbers are $(4.2,\ 2.7,\ 1.7)\times 10^{-5}$. Up to now, we have discussed the effective gluon–gluon luminosity. However, NNLO corrections may occur in the $gg \to h$ fusion vertex. These give an extra uncertainty of $\pm 20\%$. Note that we have already accounted for the NLO corrections for this vertex [10].

Furthermore, we need to consider the soft rescattering which leads to a rather small probability, $S^2 = 0.026$, that the rapidity gaps survive the soft pp interaction, see Fig. 5(b). From the analysis [36] of all soft pp data we estimate the accuracy of the prediction for S^2 is $\pm 50\%$. One check of the eikonal model calculations of S^2 is the estimate of the diffractive dijet production rate measured by the CDF collaboration [37] at the Tevatron. The rate, when calculated using factorization and the diffractive structure functions obtained from HERA data, lies about a factor of 10 above the CDF data. However, when rescattering corrections are included, and the survival probabilities computed, remarkably good agreement with the CDF measurements is obtained [38].

Combining together all these sources of error we find that the prediction for the 0^+ cross section is uncertain to a factor of almost 2.5, that is up to almost 2.5, and down almost to 1/2.5, times the default value.[11] On the other hand, 0^- production is uncertain by this factor just from the first (infrared) source of error, with the remaining errors contributing almost another factor of 2.5.

5 Simplified formulae for the CEDP signal and background

Here we give simple approximate formulae for the cross sections for the central exclusive diffractive production of $h(0^\pm)$ bosons, $pp \to p + h + p$, and for the QCD $b\bar{b}$ background as a function of mass. As was shown in Ref. [10], the cross section may be written as the product of the effective gluon–gluon luminosity $\mathcal{L}$ and the cross section for the hard subprocess $\hat{\sigma}$

$$\sigma_{\rm CEDP} = \mathcal{L}\hat{\sigma}. \tag{15}$$

At the LHC energy, the luminosity, integrated over rapidity, may be approximated, to an accuracy of better than 10% in the interval $25 < m < 250$ GeV, by

$$\frac{d\mathcal{L}}{d\ln m^2} = \int \frac{d\mathcal{L}}{dyd\ln m^2}\,dy = \begin{cases} \dfrac{9.1\times 10^5\,\langle S^2\rangle_{0^+}}{(16+m)^{3.3}} & \text{for } h(0^+) \text{ production} \\ \dfrac{1.94\times 10^3\,\langle S^2\rangle_{0^-}}{(0.5+m)^{3.45}} & \text{for } h(0^-) \text{ production} \end{cases} \tag{16}$$

[11] For example, we predict the cross section for the exclusive diffractive production of a Standard Model Higgs at the LHC, with $m_h = 120$ GeV, to be 2.2 fb with an uncertainty given by the range 0.9–5.5 fb.

where the mass m is in GeV. The factors $\langle S^2 \rangle$, which are the probability that the rapidity gaps survive the soft rescattering, are 0.026 and 0.087 for $h(0^+)$ and $h(0^-)$ respectively. The 0^- amplitude contains the kinematic factor $\vec{p}_{1\perp} \times \vec{p}_{2\perp}$, which implies that in impact parameter space the Fourier transform contains the factor $\vec{b}_{1\perp} \times \vec{b}_{2\perp}$ [9]. Thus the 0^- amplitude tends to populate larger impact parameters, where the suppression caused by soft rescattering is less effective, than does the 0^+ amplitude. The $gg \to h$ subprocesses cross section is, in the zero width approximation,

$$\hat{\sigma}_h = \frac{2\pi^2 \Gamma(h \to gg)}{m_h^3} \, \delta\left(1 - \frac{m^2}{m_h^2}\right) \; \sim \; \alpha_S^2(m_h^2) G_F, \tag{17}$$

where G_F is the Fermi constant.

The $b\bar{b}$ background processes were discussed in detail in Ref. [11] for a Standard Model $h \to b\bar{b}$ signal, with $m_h = 120$ GeV. There were four appreciable sources of $b\bar{b}$ background, each with a background-to-signal ratio in the range $B/S = 0.06$–0.08, after the appropriate cuts. In brief, these give contributions to the background subprocess cross sections of the following approximate forms

(i) $gg^{PP} \to gg$ ($b\bar{b}$ mimicked by gg): $\hat{\sigma} \sim \alpha_S^2/m^2$,

(ii) $gg^{PP} \to b\bar{b}$ ($J_z = 2$ admixture): $\hat{\sigma} \sim \alpha_s^2/m^2$,

(iii) $gg^{PP} \to b\bar{b}$ ($m_b \neq 0$, $J_z = 0$ contribution): $\hat{\sigma} \sim \alpha_S^2 m_b^2/m^4$,

(iv) NLO $gg^{PP} \to b\bar{b}g$ contribution: $\hat{\sigma} \sim \alpha_S^3/m^2$,

where the renormalisation scale is specified by $\alpha_S(m^2/4)$. The PP superscript is to denote that each incoming gluon to the hard subprocess belongs to a colour-singlet t-channel state, see Fig. 5. Note that all background contributions go like $\hat{\sigma} \sim 1/m^2$, except for (iii). In addition, for fixed missing mass resolution Δm, the background contains a factor $\Delta m/m$. Thus for large $m > 100$ GeV the background cross section behaves roughly as

$$\sigma_B = \mathcal{L}\hat{\sigma}_B \sim \Delta m/m^6, \tag{18}$$

while the Higgs signal behaves as

$$\sigma_h = \mathcal{L}\hat{\sigma}_h \sim 1/m^3. \tag{19}$$

To obtain a more precise behaviour one can use (16).

In Ref. [11] we found a signal-to-background ratio $S/B \sim 3$ for a $m_h = 120$ GeV Standard Model Higgs boson. The ratio may, however, be appreciably enhanced for SUSY Higgs with large m, and/or large $\tan\beta$. It is interesting to note that, in the region where the background is larger than the signal ($B > S$), the statistical significance of the signal $S/\sqrt{S+B} \sim m^{-3}/\sqrt{\Delta m/m^6}$ is practically independent of mass, assuming that the experimental resolution Δm is mass independent. Moreover, for a low mass, where $b\bar{b}$ pairs in the $J_z = 0$ state, (iii), give the dominant contribution to the background, the statistical significance increases with mass, as here $B \sim \Delta m/m^8$.

Finally, it is important to note that there are still various open questions which must be addressed by experimentalists in order to establish the feasibility of CEDP for Higgs searches at the LHC. One of the most challenging issues concerns triggering. Assuming that the trigger is based on the central detector only, the main task is to reduce the rate of triggering jets in order not to reach saturation of the trigger. We present below some numbers which may be useful when considering this issue.

Based on the results of Ref. [10], we see that the cross section for the CEDP of dijets with $E_T > 30$ GeV is 200 pb. If we assume that the proton tagging efficiency is 0.6, then this yields 0.12 events/sec for a luminosity of 10^{33} cm^{-2}sec^{-1}. At the same time, the inclusive cross section for production of a pair of jets, each with $E_T > 30$ GeV is about 50 μb. This leads to 50,000 events/sec, which greatly exceeds the trigger saturation limit. For CMS, for example, this latter limit is 100 events/sec [39]. Therefore it appears necessary to devise additional topological requirements in the level-1 trigger for the exclusive signal, such as making use of the presence of the rapidity gaps.

6 Identifying the pseudoscalar boson, A

If the exclusive diffractive cross sections for scalar and pseudoscalar Higgs production were comparable, it would be possible to separate them readily by the missing mass scan, and by the study of the azimuthal correlations between the outgoing proton momenta. However, we have seen that the cross section for pseudoscalar Higgs exclusive production is, unfortunately, strongly suppressed by the P-even selection rule, which holds for CEDP at LO. For values of $\tan\beta \sim 10$–15, the separation between the H/h and A bosons is much larger than their widths, see Fig. 4(d). Hence it might be just possible to observe the pseudoscalar in CEDP. For example, for $\tan\beta = 15$ and $m_A = 95$ GeV, the mass separation, 3.6 GeV, between h and A is about 8 times larger than the width Γ_h. The cross section

$$\mathrm{Br}(A \to b\bar{b}) \cdot \sigma_A \simeq 0.15 \text{ fb}, \tag{20}$$

when allowing for the large uncertainties in σ_A, could be just sufficient to bring the process to the edge of observability.

On the other hand, one may consider the semi-exclusive process

$$pp \to p + j\phi j + p, \tag{21}$$

where the Higgs bosons, $\phi = H, A$, are accompanied by two gluon jets with transverse momenta $p_\perp$ satisfying $m_\phi \gg p_\perp \gg 1$ GeV. The emission of soft gluons, with energies (in the ϕ rest frame) $E \ll m_\phi/2$, does not affect the P-even selection rule. Thus in this region the scalar H boson will be dominantly produced in process (21).

On the other hand, in the domain

$$x_i \equiv 2E_i/m_\phi \sim 1 \tag{22}$$

we lose the selection rule and have comparable H and A production. Moreover the azimuthal angular distribution[12] for the gluon jets is different for the H and A cases. In particular, for gluons with $x_1 = x_2 = 1$ accompanying A production, the azimuthal distribution is practically flat (at LO), whereas for H production it has the form $3 + 2\cos(2\phi)$. This observation may be used to distinguish between H and A production, and to study better the properties of the A boson.

Of course, we have to pay a price, of about a factor 1/20, to produce two extra jets with $p_\perp$ in the range $m_\phi \gg p_\perp \gg 1$ GeV, in a rapidity interval with $\Delta \ln x_i \sim 1$. However, this is less than the suppression of A production by the P-even selection rule. For $\tan\beta \geq 30$ and $m_A < 200$ GeV the cross section still exceeds 1 fb.

To gain more insight, it is informative to return to the original central exclusive diffractive process, which we sketch in Fig. 5(a). In the equivalent gluon approximation, the polarization vectors $\vec{\epsilon}_i$ of the gluons, carrying momentum fractions x_i, are aligned along the corresponding gluon transverse momenta $(Q-p_1)_\perp$ and $(Q+p_2)_\perp$. For very forward protons with $p_{i,\perp} \ll Q_\perp$, this leads to a correlation between the polarization vectors, namely $\vec{\epsilon}_1$ is parallel to $\vec{\epsilon}_2$. On the other hand, the ϕ production vertices behave as $V(0^+) \sim \vec{\epsilon}_1 \cdot \vec{\epsilon}_2$ and $V(0^-) \sim \vec{\epsilon}_1 \times \vec{\epsilon}_2$. Therefore the exclusive diffractive production of the pseudoscalar A boson is strongly suppressed[13].

To change the t-channel gluon polarization we need particle emission. The best possibility would be to emit either a η' or a η_c 0^- meson. Unfortunately the corresponding cross sections are too low. We lose more than a factor of 10^{-4}, which is a stronger suppression than that coming from the P-even, $J_z = 0$ selection rule. For this reason we considered the possibility of emitting a (colour singlet) pair of gluons, that is process (21). For 'soft' ($x_i \ll 1$) emission, the dominant contribution comes from the term in the triple-gluon vertex which contains $g^{\nu\nu'}$, and so does not change the gluon polarization vector. Here the indices ν and ν' correspond to the t-channel gluon polarization before and after the emission of the s-channel gluon. However for large $x_i > 1$ the major contribution comes from the term with $g^{\nu\mu}$, where μ is the s-channel gluon polarization index. In this case after the emission, the new t-channel polarization vector is directed along the new transverse momentum

[12] The possibility to discriminate the CP-parity of different Higgs states by measuring the azimuthal correlations of the two tagged gluon jets in inclusive ϕgg production was mentioned in Ref. [40]. However, the proof of the feasibility of such an approach in non-diffractive ϕgg production requires further study of the possible dilution of the effect caused by parton showers (see also [41]). An exclusive environment of the jets may be needed.

[13] However, when the polarisation vectors $\vec{\epsilon}_i$ are parallel to $\vec{Q}_\perp$, it follows, after integration over the azimuthal angle of $\vec{Q}_\perp$, that the LO QCD production of $b\bar{b}$ pair is also suppressed by a factor $(m_b/E_T)^2$; which results in a very low QCD $b\bar{b}$ background to the CEDP.

$Q'_\perp \simeq -p_\perp$. Thus for $x_i \sim 1$ the cross sections for H and A production are comparable, but now the LO QCD background is no longer suppressed.

Maybe the best chance to identify the $A(0^-)$ boson is to observe the double-diffractive inclusive process

$$pp \to X + \phi + Y, \tag{23}$$

where both protons are destroyed. In terms of t-channel gluon polarization, this is equivalent to the limit $x_i \gg 1$ in the previous reaction (21). Process (23) has the advantage of a much larger cross section[14]. However, just as for the above semi-exclusive process, we do not have the $J_z = 0$ selection rule to suppress the $b\bar{b}$ background, nor do we have the possibility of the good missing mass resolution[15]. On the other hand, the gg^{PP} luminosity is more than order of magnitude larger than for the pure exclusive case. For example, for double-diffractive inclusive production, with the rapidity gaps $\Delta\eta > 3$, the luminosity is 20 times larger than that for the exclusive diffractive production of a Higgs boson with mass $m_H = 120$ GeV (see for details [10]). So, even for the $\tau\tau$ decay mode we expect a cross section, $\sigma_{\rm incl}$, of about 20 fb for A production in the MSSM with $\tan\beta = 30$ and $m_A = 120$ GeV. This looks promising, provided that the probability for gluon misidentification as a τ is less than 1/150, which appears to be feasible[17, 42].

Despite the QCD background, the observation of the A boson also appears to be feasible for the $b\bar{b}$ decay mode, since then $\sigma \sim 200$ fb which gives a signal-to-background ratio of $S/B = 1/24$. We have evaluated the QCD $b\bar{b}$ background using the LO formula for the $gg^{PP} \to b\bar{b}$ cross section (without any K factor) with the polar angle cut $60^\circ < \theta < 120^\circ$ as was done in [11], and assumed a mass resolution of $\Delta M = 10$ GeV. The efficiency of tagging the b jets was taken to be about 0.6 [11]. This results in a statistical significance[16] of the signal for the A boson of $S/\sqrt{S+B} \sim 8.5\sigma$, for an integrated luminosity of 30 fb^{-1}. Moreover one can measure the azimuthal angle φ between the transverse energy $\vec{E}_T$ flows in the forward and backward regions, that is between the total transverse momenta of the X and Y systems. The angular dependence is driven by the momenta transferred across the rapidity gaps, and has the form

$$\begin{aligned} & \cos^2\varphi \qquad \text{for } H(0^+) \\ \text{and} \quad & \sin^2\varphi \qquad \text{for } A(0^-), \end{aligned}$$

whereas for the QCD $b\bar{b}$ background the φ dependence is flat (if we neglect the quark mass ($m_b \ll M_{b\bar{b}}/2$) and average over the b-jet momentum direction; see Eq.(15) of [43] for $Q = 0$). Thus we may suppress the $H(0^+)$ signal by selecting events with φ close to $\pi/2$. We emphasize that here we deal with rather large E_T jets, $E_T \sim 5 - 20$ GeV, and so the angular dependences are largely insensitive to the soft rescatterings. Furthermore, instead of measuring the $\vec{p}_T$ of the jets (as in Ref.[40]), for process (23) it is enough to measure the total transverse energy $\vec{E}_T$ in the forward (and backward) regions of proton dissociation.

Recall that the effective gg^{PP} luminosity for the inclusive process (23) was evaluated using the leading order formula. Thus we cannot exclude rather large NLO corrections, particularly for the non-forward BFKL amplitude. On the other hand, here, we do not enter the infrared domain. Moreover, with "skewed" kinematics, the NLO BFKL corrections are expected to be much smaller than in forward case. So we may expect that the uncertainty of the prediction is about factor of 3 - 4 (or even better).

7 Conclusion

The Central Exclusive Diffractive Processes promise a rich physics menu for studying the mechanism of electroweak symmetry breaking, and the detailed properties of the Higgs sector. We have seen, within MSSM, that the expected CEDP cross sections are large enough, especially for large $\tan\beta$, both in the intense coupling and

[14] Note that instead of the factors $1/b$, which came from the $t_i = -p_{i\perp}^2$ integrals limited by the proton form factors, as in (10) (see also eq.(8) in Ref.[10]), here we have logarithmic dt_i/t_i integrals over the intervals $Q_\perp^2 \ll |t_i| \ll m_\phi^2$. Moreover, the Sudakov supression (which arises from the requirement that no extra relatively 'hard' gluons are emitted with transverse momenta $k_\perp$ in the interval $|\vec{Q}_\perp \pm \vec{p}_{i\perp}| \ll k_\perp \ll m_\phi/2$) is much weaker than for the exclusive process due to the larger values of $p_{i\perp}$, see [10, 29]. Therefore the effective gg^{PP} luminosity for double-diffractive inclusive production is much larger than in the CEDP case.

[15] Also, in this case, pile-up can cause problems.

[16] If we include a K factor, $K \sim 1.5$, for the background then the statistical significance is about 7σ.

the decoupling regimes. Thus CEDP offers a way to cover those regions of MSSM parameter space which may be hard to access with the conventional (semi) inclusive approaches. This considerably extends the physics potential of the LHC and may provide studies which are complementary, both to the traditional non-diffractive approaches at the LHC, and to the physics program of a future Linear e^+e^- collider. To some extent this approach gives information which otherwise may have to await a Linear e^+e^- collider.

Acknowledgements

We thank Alfred Bartl, Albert De Roeck, Abdelhak Djouadi, Howie Haber, Leif Lonnblad, Walter Majerotto, Risto Orava, Andrei Shuvaev, Michael Spira, and especially Sasha Nikitenko and Georg Weiglein, for useful discussions. ADM thanks the University of Canterbury (New Zealand) for an Erskine Fellowship and the Leverhulme Trust for an Emeritus Fellowship. This work was supported by the UK Particle Physics and Astronomy Research Council, by grants INTAS 00-00366, RFBR 01-02-17383 and 01-02-17095, and by the Federal Program of the Russian Ministry of Industry, Science and Technology 40.052.1.1.1112 and SS-1124.2003.2.

References

[1] D. Cavalli et al., arXiv:hep-ph/0203056.
A. Djouadi, arXiv:hep-ph/0205248, hep-ph/0303097;
R. Harlander and W. Kilgore, arXiv:hep-ph/0305204.

[2] CMS Collaboration, Technical Proposal, report CERN/LHCC/94-38(1994);
ATLAS Collaboration, Technical Design Report, CERN/LHCC/99-15(1999);
D. Denegri et al., arXiv:hep-ph/0112045;
B. Mellado, for CMS and ATLAS Collaborations, arXiv:hep-ex/0211062.

[3] M. Carena and H. Haber, Prog. Part. Nucl. Phys. **50** (2003) 63;
G. Degrassi, S. Heinemeyer, W. Hollik, P. Slavich and G. Weiglein, Eur. Phys. J. **C28** (2003) 133

[4] S. Heinemeyer, W. Hollik and G. Weiglein, Eur. Phys. J. **C9** (1999) 343;
M. Carena et al, Nucl. Phys. **B580** (2000) 29.

[5] LEP Higgs Working Group for Higgs boson searches Collaboration, Phys. Lett. **B565** (2003) 61; arXiv:hep-ex/0107030.

[6] M. Carena, J.R. Ellis, S. Mrenna, A. Pilaftsis and C.E. Wagner, Nucl. Phys. **B659** (2003) 145, and references therein.

[7] L. Randall and R. Sundrum, Phys. Rev. Lett. **83** (1999) 3370; ibid., 4690;

[8] D. Dominici, B. Grzadkowski, J.F. Gunion and M. Toharia, arXiv:hep-ph/0206192 and references therein.

[9] A.B. Kaidalov, V.A. Khoze, A.D. Martin and M.G. Ryskin, arXiv:hep-ph/0307064.

[10] V.A. Khoze, A.D. Martin and M.G. Ryskin, Eur. Phys. J. **C23** (2002) 311.

[11] A. De Roeck, V.A. Khoze, A.D. Martin, R. Orava and M.G. Ryskin, Eur. Phys. J. **C25** (2002) 391.

[12] E. Boos, A. Djouadi, M. Mühlleitner and A. Vologdin, Phys. Rev. **D66** (2002) 055004.

[13] E. Boos, A. Djouadi and A. Nikitenko, arXiv:hep-ph/0307079.

[14] A.D. Martin, R.G. Roberts, W.J. Stirling and R.S. Thorne, Eur. Phys. J. **C14** (2000) 133.

[15] A. Djouadi, J. Kalinowski and M. Spira, Comput. Phys. Com. **108** (1998) 56, arXiv:hep-ph/9704448.

[16] S. Heinemeyer, W. Hollik and G. Weiglein, arXiv:htp-ph/0002213.

[17] D. Cavalli et al., ATLAS Internal note, PHYS-NO-051, 1994;
R. Kinnunen and A. Nikitenko, CMS Note 1997/002.

[18] V.A. Khoze, A.D. Martin and M.G. Ryskin, hep-ph/0006005, in *Proc. of 8th Int. Workshop on Deep Inelastic Scattering and QCD (DIS2000)*, Liverpool, eds. J. Gracey and T. Greenshaw (World Scientific, 2001), p.592.

[19] V.A. Khoze, A.D. Martin and M.G. Ryskin, Nucl. Phys. Proc. Suppl. **99B** (2001) 188.

[20] V.A. Khoze, A.D. Martin and M.G. Ryskin, Eur. Phys. J. **C19** (2001) 477, erratum **C20** (2001) 599.

[21] Review of Particle Physics, K. Hagiwara et al., Phys. Rev. **D66** (2002) 010001.

[22] see, for example, H.E. Haber, published in Ringberg Electroweak Workshop 1995, 219–232, arXiv:hep-ph/9505240;
J.F. Gunion and H.E. Haber, Phys. Rev. **D67** (2003) 075019.

[23] B.E. Cox, J.R. Forshaw, J.S. Lee, J. Monk and A. Pilaftsis, arXiv:hep-ph/0303206;
J.R. Forshaw, hep-ph/0305162.

[24] J. Ohnemus, T.F. Walsh and P.M. Zerwas, Phys.Lett. **B328** (1994) 369.

[25] K. Piotrzkowski, Phys. Rev. **D63** (2001) 071502; arXiv:hep-ex/0201027.

[26] V.A. Khoze, A.D. Martin and M.G. Ryskin, Eur. Phys. J. **C24** (2002) 459.

[27] V.A. Khoze, A.D. Martin and M.G. Ryskin (in preparation).

[28] T. Ibrahim and P. Nath, Phys. Rev. **D68** (2003) 015008.

[29] V.A. Khoze, A.D. Martin and M.G. Ryskin, Eur. Phys. J. **C14** (2000) 525.

[30] V.A. Khoze, A.D. Martin and M.G. Ryskin, Phys. Lett. **B401** (1997) 330.

[31] M. Spira, A. Djouadi, D. Graudenz and P.M. Zerwas, Nucl. Phys. **B453** (1995) 17.

[32] A.D. Martin and M.G. Ryskin, Phys. Rev. **D64** (2001) 094017.

[33] A.G. Shuvaev, K.J. Golec-Biernat, A.D. Martin and M.G. Ryskin, Phys. Rev. **D60** (1999) 014015.

[34] CTEQ Collaboration: J. Pumplin et al., JHEP **0207** (2002) 012.

[35] A.D. Martin, R.G. Roberts, W.J. Stirling and R.S. Thorne, Eur. Phys. J. **C28** (2003) 455.

[36] V.A. Khoze, A.D. Martin and M.G. Ryskin, Eur. Phys. J. **C18** (2000) 167.

[37] CDF Collaboration: T. Affolder et al., Phys. Rev. Lett. **85** (2000) 4215.

[38] A.B. Kaidalov, V.A. Khoze, A.D. Martin and M.G. Ryskin, Eur. Phys. J. **C21** (2001) 521.

[39] CMS Collaboration, The Data Acquisition and High Level Trigger Project, Technical Design Report, CERN/LHCC 2002-26, CMS TDR 6.2, (2002).

[40] V. Del Duca, W. Kilgore, C. Oleari, C. Schmidt and D. Zeppenfeld, Nucl. Phys. **B616** (2001) 367; Phys. Rev. Lett. **87** (2001) 122001.

[41] K. Odagiri, JHEP **0303** (2003) 009.

[42] D. Rainwater, D. Zeppenfeld and K. Hagiwara, Phys. Rev. **D59** (1999) 014037.

[43] V.A. Khoze, A.D. Martin, R. Orava and M.G. Ryskin, Eur. Phys. J. **C19** (2001) 313.